



Biodegradability of tomato stem-reinforced composites: Towards a virtuous approach to local and circular waste upcycling

Estelle Bonnin^{a,*} , Méline Calatraba^{a,1}, Xavier Gabrion^b , Camille Alvarado^a, Coralie Buffet^c, Arnaud Day^{d,e} , Lèna Brionne^a, Alain Bourmaud^c, Johnny Beaugrand^a

^a INRAE, UR BIA Biopolymères Interactions Assemblages, F-44316 Nantes, France

^b SupMicroTech-ENSMCM, CNRS, Institut FEMTO-ST, F-25000 Besançon, France

^c Univ. Bretagne Sud, UMR CNRS 6027, IRDL, F-56100 Lorient, France

^d Fibres Recherche Développement, Technopole de l'Aube en Champagne, CS 90601, F-10900 Troyes, France

^e Univ. Lille, UMR CNRS 8576 – UGSF, F-59000 Lille, France

ARTICLE INFO

Keywords:

Biopolymers
Fiber
Enzymatic degradability
Tomography
Eco-material

ABSTRACT

The current method of producing tomatoes in greenhouses uses petro-sourced plastic accessories that contaminate plant waste when the greenhouses are emptied. For this reason, this study aims to develop a biodegradable material to replace plastic accessories. To evaluate the feasibility of using tomato byproduct as reinforcements in a range of bio-based and biodegradable thermoplastic materials, the compound degradability was investigated through biochemical and imaging approaches. The first set of experiments carried out on the tomato stem showed that the enzymatic degradation by a mixture of cellulases and pectinases efficiently removed constitutive biopolymers, and that the average size and the polydispersity decreased during treatment. The largest particles became more irregular, highlighting the enzyme-recalcitrant domains. When compounded with different matrix polymers (PBS, PBAT/PHA or PBAT/PLA), tomato stem particles remained susceptible to enzymatic degradation. Tomography analysis showed that all the degraded samples exhibited a large increase in porosity, the largest increase being observed in the PLA-containing specimens.

This fully circular approach from waste to useful compounds for horticulture and market gardening is a promising way of upcycling tomato biomass, compatible with end-of-life composting.

Introduction

Synthetic fibers such as ceramic, carbon or glass fibers are widely used in the reinforcement of composites (Rani et al., 2021; Al-Furjan et al., 2022). However, their nonbiodegradability means that they must be disposed of by recycling, if recycling channels exist, or otherwise by pyrolysis or combustion. Therefore, these fibers emit significant amount of greenhouse gases during production, and again at end-of-life. By contrast, plant fibers are derived from renewable resources, and their use as a replacement for synthetic fibers is receiving increasing attention. Environmentally speaking, these materials are also of great interest; for example, the production of scutched flax fibers is approximately 4 times less energy intensive than that of glass fibers (Le Duigou et al., 2011). Plant fibers are efficient at providing composite reinforcement (Coroller et al., 2013). However, their great variability in composition,

structure and biodegradability, especially when they are not protected by a polymer matrix, is an obstacle to their use. Therefore, additional work and research on their characterization should be performed.

European production is rather stable at approximately 20.5 M tons of tomato in 2022 (www.fao.org), behind the largest producers that are China (68.2 M tons) and India (20.7 M tons). France is the 4th European tomato producer with 711,000 tons in 2022, including 504,250 tons cultivated in greenhouses (Eurostat, 2024). Tomato stems and leaves are the post-harvest biomass remaining from greenhouses after the period of tomato production, and thus are waste biomass fibers, as defined by Shadhin et al. (2023). The ratio between tomato fruit and aerial biomass (which includes leaves, stems, and non-harvested parts of the plant) can vary significantly depending cultivation conditions (Deram et al., 2014). In average, the non-harvested biomass represents approximately 1/5 of the usable production.

* Corresponding author.

E-mail address: estelle.bonnin@inrae.fr (E. Bonnin).

¹ Present address: IFREMER, EM3B, F-44311 Nantes, France

<https://doi.org/10.1016/j.clcb.2025.100136>

Received 10 April 2024; Received in revised form 9 January 2025; Accepted 11 January 2025

Available online 16 January 2025

2772-8013/© 2025 The Authors. Published by Elsevier Ltd. This is an open access article under the CC BY license (<http://creativecommons.org/licenses/by/4.0/>).

The current method of growing tomatoes in greenhouses consumes many plastic accessories that are almost exclusively produced from petro-sourced and nondegradable polymers, such as the string to lead the stem, the clips to fix the stem on the string and the bouquet holders to reinforce the peduncle. One hectare of greenhouse needs approximately 500,000 clips and 500,000 bouquet holders / harvest, representing approximately 1 ton/ha. The presence of plastic pieces contaminates the non-harvested biomass and prevents the composting of plant waste after greenhouses are emptied. As a first detrimental consequence, treatment costs are assumed by market gardeners: 120 euros/ton for landfill and 100 €/t for incineration (excluding transport; ADEME 2020). As a second detrimental consequence, the presence of plastic pieces in the biomass causes the biomass to be classified as ordinary waste and prevents it from being used in a circular economy. A circular bioeconomy in which this biomass can be recycled is desirable, but first requires the development of biodegradable pieces. The European surface of tomato greenhouses reaches 60,000 ha (Eurostat, 2024). In France, the area devoted to tomato cultivation is rather stable (2120 ha in 2023, - 1.7 % compared to the average 2018–2022, Eurostat, 2024), with high production density in a small geographical area, facilitating collection and the potential for further processing at the local level with minimal transport costs.

In the same philosophy of eco-design to make the most from tomato stems, their upcycling and local use has led to investigate diversified uses such as “Packaging” or “Boards, panels and blocks” (Manriquez-Altamirano et al., 2021). In composite films with synthetic polymers from fossil sources such as poly(vinyl alcohol-co-ethylene), post-harvest tomato plant powder may be suitable as filler (Nistico et al., 2017). Moreover, biobased or biodegradable materials reinforced by tomato stem particles exhibit mechanical properties that can easily compete with flax-reinforced composites already used in automotive industry (Bourmaud et al., 2023). Also, the interest of tomato particles was shown for designing new compos Table 3D printing filaments (Pemas et al., 2024, Scaffaro et al., 2023), notably with particular application such as controlled soil fertilization and copper removal (Scaffaro et al., 2024). The main polymers identified in tomato stems are cellulose, pectin and lignin (Bourmaud et al., 2023), which are substrates of the numerous polysaccharides-degrading enzymes and lacases produced at different levels by the compost microorganisms (Santos-Pereira et al., 2023). Even though lignocellulose exhibits a partial recalcitrance, bacteria and filamentous fungi in nature produce an arsenal of hydrolases and oxidases able to degrade lignocellulose (Yadav, 2017). This suggests that the presence of tomato biomass in composites will improve its degradability, and that this phenomenon can be monitored by following the evolution of the sugar fraction in the composites.

X-ray computed tomography (XCT) is an interesting nondestructive inspection technique for measuring 3D phenomena in composites or natural materials, such as porosity and cracking (Garcea et al., 2018; Zwanenburg et al., 2023), adsorption mechanisms and microstructures (Jiang et al., 2018; Mongioli et al., 2021, 2022) or defects (Beaugrand et al., 2017; Bourmaud et al., 2022; Quereilhac et al., 2023). Tomography has been used on biobased composites for exploring pore size and distribution. Indeed, most of the commonly used thermoplastic polymers have sufficient density contrast with plant cell walls to obtain relevant results. In particular, Pantaloni et al. (2020) explored the microstructure of flax-reinforced degradable composites using a range of matrices, i.e., poly-hydroxy alkanooate PHA, poly-lactic acid PLA and poly-butylene succinate PBS. The authors demonstrated that the degradation mechanism was very different according to the matrix considered. For the PBS and PHA composite materials, the surface of the samples was more degraded. Conversely with PLA, the degradation was more effective in the sample volume and at the fiber-matrix interface.

The aim of the present study was to investigate the enzymatic susceptibility of tomato stems used as fillers in degradable polymers to anticipate the biodegradability of tomato stem-reinforced composites

during aging processes, such as home composting. By elucidating the interplay between substrate composition, enzyme action and enzyme-induced porosity, this study seeks to provide valuable insights that are applicable to the production of biobased cultivation accessories, in order to develop more eco-responsible tomato production methods by integrating tomato biomass to produce biodegradable composite accessories that can replace fossil resource-based plastic accessories in a virtuous circular bioeconomy.

Materials and methods

Plant material

The tomato biomass was collected in the Brittany region (France) at the end of the greenhouse cultivation (Savéol, Plougastel-Daoulas, France, 2019). The batch contained approximately 5 % by weight plastic accessories that were manually removed. The plant material recovered contained 93 % weight stem and 7 % weight leaves. The sample was dried for 12 h at 60 °C, and subsequently crushed with a hammer miller equipped with a 1000 µm grid.

Polymers used as composite matrix

PBS (BioPBSTM FZ71PM, PPT MCC Biochem, Thailand), PHA (PHI 002, Natureplast), and PLA (PLI 005, NaturePlast) and PBAT (PBE 006, NaturePlast) polymers were used. The melt flow indices (MFIs) are 22, 15–30, 25–35 and 4–6 g/10 min (2.16 kg, 190 °C), respectively.

Enzymes used as biodegradation agents

The multienzyme commercial preparations Cellic CTec2 and Rapidase Fiber were kindly provided by Novozymes A/S (Bagsvaerd, Denmark) and DSM (Delft, The Netherlands), respectively. The former was produced by *Trichoderma reesei*, and the latter was generated from selected strains of *Aspergillus niger* and *Trichoderma longibrachiatum*. The protein content and activities are shown in Table 1.

Enzymatic degradation

Fifty milligrams of tomato powder was suspended in deionized water. The controls without enzymes and the assays with enzymes were incubated overnight at 40 °C on a rotary wheel at 20 rpm. The volume of enzymes containing 0.5 mg of protein was calculated. To test the effect of the mixture of the enzymatic preparations, the volume of each preparation was calculated to reach 0.25 mg of protein. Assays and controls were incubated in duplicate.

Biochemical characterization

The dry matter and ash content were determined via thermogravimetric analysis on a TGA 2050 instrument (TA instrument, Newcastle, DE, USA) controlled by TA Instrument Control software following a heating rate of 10 °C/min up to 550 °C. Analyses were performed in duplicate.

The neutral sugar composition was established after prehydrolysis in 12 M sulfuric acid (30 min, 25 °C) and then hydrolysis in 1 M sulfuric acid (2 h, 100 °C). Sugars were reduced, acetylated and analyzed as alditol acetates by gas-liquid chromatography (Englyst and Cummings, 1988) on a PerkinElmer AutoSystem (France) mounted with a DB 225 capillary column (J & W Scientific, Folsom, CA, USA; temperature 205 °C, carrier gas H₂). Inositol was added as the internal standard and a standard solution of sugars was used for calculation of individual response factors. The results were compared with those obtained without prehydrolysis to quantify the cellulose content. Analyses were performed in triplicate.

The uronic acid content was measured after hydrolysis by

Table 1

Protein content and main activities measured in Cellic CTec2 and Rapidase Fiber. PL, pectin lyase; PG, polygalacturonase; RGase, rhamnoglucuronase; XGase, xyloglucanase; CMCase, carboxymethylcellulase. N/A, not appropriate.

| | Protein (mg/mL) | PL | PG | RGase | Arabinanase (nkat/mL) | Galactanase | XGase | Xylanase | CMCase |
|-----------------------|--------------------|-----|------|-------|--------------------------|-------------|-------|----------|--------|
| Cellic CTec2 | 82.8 | N/A | N/A | N/A | N/A | N/A | N/A | 10.1 | 25.9 |
| Rapidase Fiber | 9.6 | 3.9 | 19.9 | 638 | 612 | 103 | 1.1 | 1.8 | 438 |

concentrated (18 M) sulfuric acid with or without sodium tetraborate (12.5 mM), followed by m-hydroxydiphenyl colorimetric determination (Blumenkrantz and Asboe-Hansen, 1973) as automated by (Thibault, 1979). Galacturonic acid and glucuronic acid were used as standards. Analyses were performed in triplicate. The resulting sugar composition was expressed as the anhydrous sugar content to account for the polysaccharide form in the sample.

The protein content was deduced from the determination of nitrogen content on a CNS elemental analyzer Vario (Elementar, Lyon, France). The samples were analyzed in triplicate and the conversion factor of 5.77 was used (Torabizadeh, 2011).

The acetyl bromide method was used to quantify the lignin content (Fukushima and Hatfield, 2001). Analysis was performed in duplicate.

Particle characterization during enzymatic degradation

The particle morphology was characterized using an automated dynamic morphological analyzer (QICPIC), equipped with a dispersion unit (LIXELL; SympaTec GmbH, Clausthal, Germany). The particle morphology is measured in continuous flow and is based on dynamic image analysis applied to image projections of individual particles.

PAQXOS software (SympaTec GmbH, Clausthal, Germany) was used to analyze the data and calculate the number of particles as well as various morphological features. The equal projection area of a circle (EQPC) is the diameter of a circle with an equal perimeter. The sphericity is the ratio of the EQPC divided by the real perimeter of the particle. An irregular shape induces an increase in the diameter, the smaller the sphericity is, the more irregular the particle shape.

Tomato particles (50 mg) were first suspended in ethanol in order to avoid aggregation, and the suspension was subsequently dispersed in 1 L of water. The samples were analyzed using a 2 mm cuvette, and an M7 lens, which allows measurement of size and shape in the 38 to 8665 μm range. A peristaltic pump ensured the circulation of the sample during the time course of degradation. Acquisitions were performed at 85 images/s for 300 s at 0 h, 1 h, 2 h, 4 h, 6 h, 8 h and 24 h after adding enzymes. A control sample was measured in the absence of enzyme under the same conditions and in triplicate. Finally, the number of observed particles was 32.4 million on average, with a standard deviation of 1.2 million. The repeatability of the number of particles and the repeatability of the density distribution allowed to consider that the conditions of measurement were satisfactory, notably the acquisition frequency and time.

Microscopy

Pieces of dried tomato stems were rehydrated in water by overnight incubation at 4 °C, and subsequently cut on a vibratome (HM650 V, Microm Microtech, Brignais, France) into 30 μm thick cross sections.

Fuscin–alcian blue–safranin–glycerin–aqua (FASGA) staining allows us to distinguish lignified tissues as red–pink and nonlignified or poorly lignified tissues as cyan–blue (El Hage et al., 2018). The FASGA solution was prepared by mixing 3 mL of Safranin Red solution at 1 %, 11 mL of Alcian Blue solution at 0.5 %, 30 mL of glycerin, 20 mL of ultrapure water and 1 mL of pure acetic acid. The sections were stained with the FASGA solution diluted 1/8 for 24 h at room temperature under gentle agitation. The sections were rinsed several times with ultrapure water for 24 h, under constant agitation and then mounted on glass slides for

acquisition. Images of the stained sections were observed using bright-field microscopy (DM2500 LED, Leica Microsystems, Wetzlar, Germany).

Before immunolabeling, fragments of dry tomato stems were cut with a razor blade to 1 mm³ blocks. Blocks were infiltrated with LRWhite acrylic resin (London Resin White) and polymerized for 72 h at 56 °C. Semithin sections (1 μm) were cut on an ultramicrotome (UC7, Leica Microsystems, Wetzlar, Germany). The sections were floated for 30 min at room temperature on a drop of phosphate-buffered saline supplemented with bovine serum albumin to block nonspecific labeling. The sections were further incubated with two primary antibodies (LM19, specific for low methoxy pectin; LM25 specific for galactosylated xyloglucan) and a carbohydrate binding module (CBM3a specific for crystalline cellulose) used at the accurate dilution. The sections were washed and incubated with a secondary antibody conjugated with the fluorescent probe Alexa Fluor 546 nm. As a control, the primary antibody was replaced with phosphate-buffered saline. The sections were labelled as is or after enzymatic treatment with 2 μg of the mixture Cellic CTec2 + Rapidase Fiber. They were observed using a fluorescence microscope (DMRB-DMRD, Leica Microsystems, Wetzlar, Germany), with an objective x20 and an acquisition time of 400 ms.

Composite manufacturing

Before processing, all the materials were dried in an oven under vacuum at 60 °C for at least 12 h. A corotating twin screw extruder (FSCM 21–40, TSA, Cernobbio, Italy) with a screw diameter of 20 mm and an L/D ratio = 40 was used for extrusion compounding. The temperature varied depending on the polymer used (PBS: 150–160 °C, PBAT/PHA: 170 °C, PBAT/PLA: 180 °C). The rotational speed was 300 rpm. Three virgin polymer blends were manufactured as references (Table 2). Using the same polymer matrix, composites reinforced with ground tomato particles were produced. A fraction of 30 % tomato particles was chosen in accordance with Bourmaud et al. (2023). The material obtained was then granulated (T5, Meccanoplastica, Castiglione Olona, Italy) and dried again at 60 °C for at least 12 h before injection molding of ISO 527 dog bone specimens (HM 80/120 E, Battenfeld Kunststoffmaschinen, Kottlingbrunn, Austria).

Tomography of tomato particles and composite samples

An EASYTOM (RX-SOLUTION, Chavanod, France) equipment was used to scan the samples. Composite specimens were taken from each dog bone sample for X-Ray imaging. Their size was 6 × 6 × 4 mm. The whole samples were scanned at a resolution of 5 μm with a voltage of 60 kV and a current of 87 μA . The number of projections was fixed at 1440

Table 2

Formulation of the composites and their tomato-reinforced counterparts, expressed in % weight.

| Sample | PBS (%) | PHA (%) | PBAT (%) | PLA (%) | Tomato stem (%) |
|------------------|------------|------------|-------------|------------|--------------------|
| PBS | 70 | 0 | 0 | 0 | 30 |
| PBAT60/ PHA40 | 0 | 28 | 42 | 0 | 30 |
| PBAT60/ PLA40 | 0 | 0 | 42 | 28 | 30 |

over 360° with an exposure time of 400 ms and an average of 5 images in start and stop mode. These parameters lead to a tomography time of 1 h per specimen.

The reconstruction was performed with X-act software (RX-SOLUTION, Chavanod, France) to extract the vertical slice with a filtered backprojection algorithm.

The data were analyzed with VG StudioMax 2023–1 Software (Heidelberg, Germany). To evaluate the degradation, the volume fraction of the pores was calculated with an algorithm implemented in the software based on the gray level. For this analysis, a special treatment of the slice was performed:

- Segmentation (based on gray level) was performed to retrieve the entire volume of the specimen.
- Extraction of region of interest (ROI).
- Successive steps of erosion (to avoid edge effects) and closing (to ensure that all porosities and cracks are in the ROI) were performed.
- Binarization of the slices was performed.
- The porosity-to-volume fraction was measured.

The porosity volume fraction was calculated as follows:

$$V_p = \frac{v_V}{v_S} * 100$$

where V_p is the porosity volume fraction, v_V is the porosity volume and v_S the specimen volume, both in mm^3 .

A piece of 165 mg of each composite specimen was plunged in 2 mL of water. The samples were incubated at 40°C on a rotary wheel at 20 rpm. A volume of fresh enzyme containing 0.5 mg of protein was added every 2 days for 3 weeks (referred to as treatment #1) and again during a second treatment period of 3 weeks (referred to as treatment #2). To evaluate the impact of the degradation on the composite samples, the same piece of each composite specimen was scanned at 3 time points: before enzymatic treatment, after the first period (treatment #1), and after the second period (treatment #2). In this way, we were able to follow the evolution of each specimen without bias from the local heterogeneity of the injected material. To strictly compare the same view in terms of orientation and direction (image), each specimen was aligned with the best fit algorithm, and the piece volumes before treatment, after treatment #1 and after treatment #2 were superimposed.

A control was carried out on another piece of each composite under the same conditions except that the reaction medium was free of enzyme.

Results and discussion

Characterization of the tomato material

The tomato sample contained mainly stems from the tomato plants harvested at the end of the production period. The fresh sample contained 49.3 % dry matter. Sugar analysis revealed that the total sugar content reached 39.8 % (Table 3). The sugar fraction consisted mainly of glucose (20.6 %). The glucose contents obtained after pre-hydrolysis and without pre-hydrolysis allowed to determine that the cellulose content reached 17.9 %. The presence of galacturonic acid and rhamnose was related to pectin, which also included some of the galactose and arabinose contents (Bonnin et al., 2014). This sugar composition indicated that the aging agent to be applied to degrade tomato stem-containing materials should consist of cellulose- and pectin-degrading enzymes.

The values obtained here are quite different from those published by Manriquez-Altamirano et al. (2021), especially for cellulose content. However, these authors also report significant differences between their different samples and do not give values for the pectic sugars.

Light microscopy observation of cross-sections revealed a typical tomato stem structure made of epidermis, cortical parenchyma,

Table 3

Overall composition (% DM): (partly from Bourmaud et al., 2023).

| | % DM |
|-----------|-------------|
| Rhamnose | 0.6 ± 0.05 |
| Arabinose | 1.5 ± 0.13 |
| Xylose | 6.0 ± 0.24 |
| Mannose | 1.6 ± 0.21 |
| Galactose | 1.5 ± 0.02 |
| Glucose | 20.6 ± 0.65 |
| GalA | 7.6 ± 0.26 |
| GlcA | 0.3 ± 0.33 |
| Lignin | 13.4 ± 0.4 |
| Protein | 11.4 ± 0.5 |
| Ashes | 19.2 ± 0.2 |
| TOTAL | 83.7 |

cambium, and phloem and xylem bundles (Fig. 1). The FASGA coloration allows polysaccharides to be distinguished as blue and lignin as dark pink. Lignin was mainly concentrated in the phloem and xylem tissues, whereas both types of polymers were present in the inner part of the cortical parenchyma.

Because the particle state impacts the enzymatic susceptibility, the tomato powder was explored using the dynamic morphological analyzer QicPic in liquid mode. The density diameter was plotted as a function of the diameter of a circle of equal perimeter (EQPC = equivalent projection area of a circle, Fig. 2A). The sample showed high heterogeneity with particle sizes between 10 and 1010 μm . The main fraction in the starting powder was in the range of 200 to 500 μm . This view allowed to define 4 subpopulations in this sample: <60 μm , 60<>150, 150<>550 and >550 μm . The aspect ratio length/width is an important parameter for the use of biomass as composite reinforcement. In the tomato stem fraction, it varied from 1.53 to 2.32, with a mean value of 1.84 for the whole population, suggesting that the particles were slightly elongated. The calculated values are in good agreement with tomography observations (Fig. 2), where both elongated and quasi-circular particles were evidenced. Compared to those of conventional biobased products used as composite reinforcements such as flax fibers or shives (Nuez et al., 2020), these values are very low but in good agreement with previously published data obtained on tomato stem particles (Bourmaud et al., 2023). To be efficient in composite materials, it is generally admitted that the aspect ratio of fibers must be above 10 to ensure efficient polymer reinforcement (Kelly and Tyson, 1965). In the present case, tomato products could provide sufficient reinforcement for low bearing applications. Nevertheless, some particles exhibited high L/D values (Fig. 2B), demonstrating the important potential of reinforcement for certain stem tissues. In a future work, it would be possible to separate particles according to their morphology to design composite materials with improved performances.

Among the interesting shape parameters for characterizing particles, the sphericity is defined as the ratio of the EQPC to the real perimeter of the particle. The value is 1 for a sphere, and the more it decreases, the more irregular the particle is. In the tomato powder, the sphericity varied between 0.9 for the smallest particles and 0.53 for the largest particles. The average value in the most representative subfraction, in the range of 150 to 550 μm , was 0.55.

The rather elongated form of the particles was confirmed by tomography, where some of the particles appeared as rods (Fig. 2B). The different macroscale structures of these particles show that they originated from different tissues of the stem and can be explained by the particular behavior of these different tissues during grinding.

Enzymatic degradation of the tomato material

The tomato stem powder was subjected to enzymatic degradation using two different enzymatic preparations, one containing cellulases and hemicellulases, and the other one containing pectin-degrading

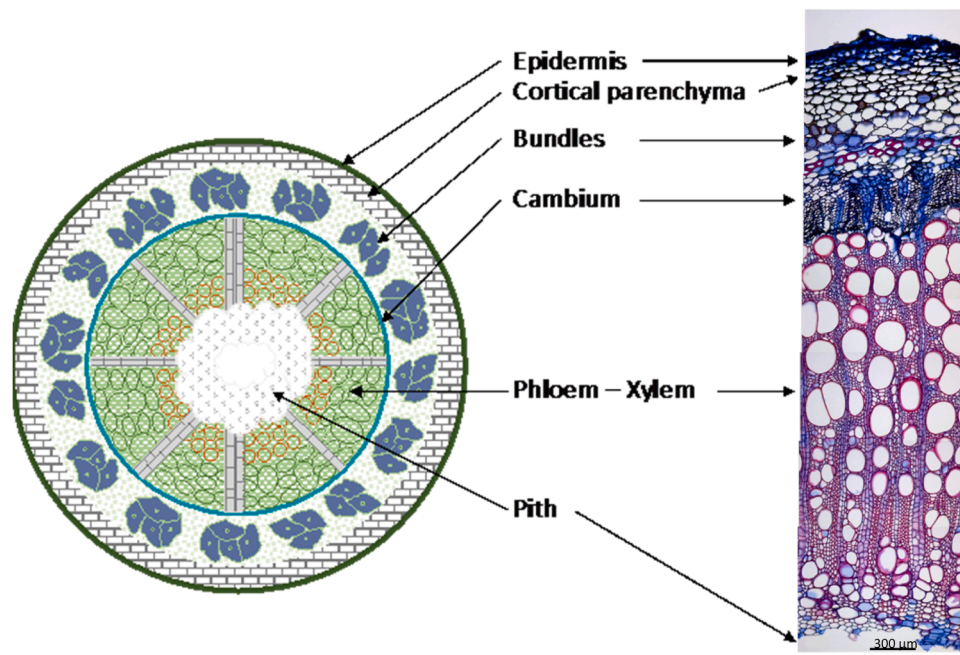


Fig. 1. Schematic representation and brightfield imaging (x10) of tomato stem after FASGA coloration. Lignified and nonlignified tissues are highlighted in red-pink and cyan-blue, respectively. Scale bar scale = 300 μm .

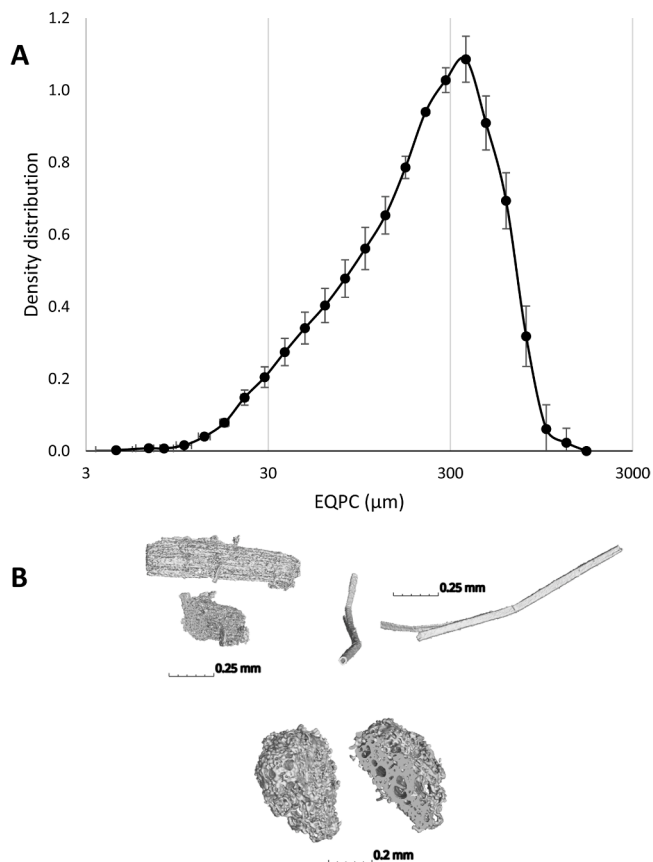


Fig. 2. A) Density distribution of the EQPC (μm) in the native fraction of tomato particles measured via a dynamic morphological analyzer. B) Images of particles randomly extracted from a general tomography view of the native tomato sample.

enzymes, namely Cellic CTec2 and Rapidase Fiber, respectively. These preparations were chosen according to the chemical characterization of the tomato powder, which exhibited a predominance of cellulose and pectin (Table 3). The preparations were tested alone and in combination, and the solubilization yields and the sugar composition of the residues were determined (Table 4).

Enzymatic treatments resulted in a 35.9 to 45.7 % loss in dry matter. Regardless of the enzyme used, arabinose was the most sensitive sugar, and xylose was the most recalcitrant. These two results are related to the high arabinanase activity in the Rapidase Fiber cocktail and the low xylanase activity in both enzymatic preparations. Xylanase activity has been previously shown to be a key feature for improving the total hydrolysis of softwood (Várnai et al., 2011).

In the presence of the enzyme mixture, the residue contained half or less of the initial content of pectic monomers (rhamnose, arabinose, galactose, galacturonic acid) as well as glucose. This difference resulted from the pectinase and cellulase activities ensured by Rapidase Fiber and Cellic CTec2, respectively.

Finally, the most efficient condition was the mixture of the two preparations, which was therefore chosen as the degradation condition for the rest of the study.

To follow the effect of the enzyme on the tomato stem tissue, labeling with affinity probes using the antibodies LM19 and LM25, and the carbohydrate-binding module CBM3a was carried out. Fig. 3 shows that low-methoxy pectin labeled by the LM19 antibody were present in all the cell types constituting the tomato stem, and that these compounds were lost after enzymatic degradation by the mixture of Cellic CTec2 and Rapidase Fiber. LM25 antibody labeling revealed that the different cell types contained galactosylated xyloglucan, and that this polysaccharide was released by the enzymes. Crystalline cellulose, labeled by the carbohydrate binding module CBM3a, was present in all the tissues, although it was not visible in the vessels. After enzymatic degradation, crystalline cellulose was more obvious, even on the vessels (Column a).

The particle size is another parameter that can be used to monitor the enzymatic degradation. Therefore, the time course of enzymatic degradation was determined using the dynamic morphological analyzer QicPic. The particle size was analyzed for the samples in which the enzyme mixture was added, and it was compared to that of the control

Table 4

Solubilization yields and sugar composition of residues after overnight enzymatic degradation, expressed as a percentage of the initial content of each sugar. The values are the average of triplicates. The standard deviations are given in brackets. Rha, rhamnose; Ara, arabinose; Xyl, xylose; Man, mannose; Gal, galactose; Glc, glucose; GalA, galacturonic acid; GlcA, glucuronic acid.

| | Yield | Rha* | Ara | Xyl | Man | Gal | Glc | GalA | GlcA* |
|-----------------------|-----------------|------------------|-----------------|-----------------|-----------------|-----------------|-----------------|-----------------|-------------------|
| Control | 30.2 (± 0.6) | 67.6 (± 10.9) | 66.5 (± 8.4) | 89.7 (± 3.5) | 66.7 (± 6.9) | 76.2 (± 3.7) | 76.6 (± 4.8) | 76.5 (± 3.9) | 69.8 (± 14.4) |
| Cellic CTec2 | 35.9 (± 0.8) | 60.1 (± 10.9) | 43.2 (± 4.6) | 82.3 (± 3.5) | 59.7 (± 7.4) | 67.5 (± 3.2) | 69.5 (± 4.6) | 66.5 (± 3.2) | 100.0 (± 10.3) |
| Rapidase Fiber | 41.7 (± 0.7) | 43.7 (± 7.6) | 27.6 (± 1.8) | 86.2 (± 5.8) | 49.9 (± 4.3) | 39.1 (± 4.6) | 62.8 (± 5.4) | 39.6 (± 3.7) | 61.7 (± 18.5) |
| Mixture | 45.7 (± 0.7) | 52.6 (± 9.8) | 44.5 (± 7.4) | 71.1 (± 4.3) | 39.4 (± 7.4) | 42.9 (± 7.8) | 51.2 (± 5.9) | 44.8 (± 5.1) | 70.3 (± 16.4) |

* Standard deviations for rhamnose and glucuronic acid are very high due to their very low content in the tomato stem (Table 3).

samples. The distribution density of EQPC remained rather stable over 24 h in the controls, whereas in the enzyme assay, the peak shifted towards the smallest sizes and the polydispersity decreased with time (Suppl. Fig. 1). The particles were separated into 4 populations of increasing sizes and the different populations were plotted as a function of time (Fig. 4). In the absence of the enzyme, the particle size distribution did not change substantially (Fig. 4A). Most of the particles were between 60 µm and 550 µm in diameter, representing 72.3 % of the sample at T0 and 76.5 % at T24. In the presence of the enzymes (Fig. 4B), the same populations represented 73.6 % of the particles at T0 vs. 86.9 % after 24 h of hydrolysis. The population of the smallest particles decreased from 18.9 % to 12 % while the population of the largest particles almost disappeared (from 7.5 % to 1 %). Simultaneously the sphericity tended to decrease when comparing T0 and T24. After degradation, the sphericity remained unchanged at 0.89 for the smallest particles, while it decreased from 0.54 to 0.32 for the largest particles. This indicates that the largest particles became highly irregular under the action of the enzymes. This difference is related to the enzymatic sensitivity of the different tissues that may be present in each particle, as highlighted in the particle images shown in the Supplementary Fig. 2. The images of individual particles also suggest that the degraded particles were less dense than the control particles, due to the loss of material.

These imaging experiments confirmed that the tomato stem was rather sensitive to the enzymatic degradation by Cellic CTec2 and Rapidase Fiber in combination. This approach allowed to quantify the degradability and identify the vessels as the most recalcitrant tissues.

Enzymatic degradation of composites

To evaluate the susceptibility of the composites, the samples were subjected to 3 weeks enzymatic degradation after grinding or not. The residues were weighed and the results were compared to those of controls carried out in the absence of enzymes (Table 5).

The fiber-free polymers were rather resistant to the degradation as their percentage of solubilization was in the same range with and without enzymes. Interestingly, the addition of plant fibers facilitated the degradation. When not ground, all samples lost more material than the polymers alone, but without any significant effect of the presence of enzymes. When the treatments were applied after grinding the composite pieces to 2 mm, the yields of solubilization of the Control assays increased likely due to an increased accessibility to the tomato particles. The increase was even higher for all samples in the presence of enzymes. *Aspergillus* fungus was previously reported to secrete an enzyme able to depolymerize biosourced polyesters, including PBS (Jung et al., 2018). However, the polymers were subjected to enzymatic degradation in the form of films, making them more accessible to the enzyme than in a fairly thick specimen. This result is in line with the difference observed in the present study between ground and unground specimens. The biodegradation of PLA-jute composites by *Aspergillus flavus* extract was more intensive than that of unblended PLA (Karimi-Avargani et al.,

2020). Plant particles may increase the diffusion of water, enzymes, fungi or bacteria, especially through their lumen (Melelli et al., 2021). The addition of plant particles increases the heterogeneity of the composite and induces the development of sensitive interfacial regions.

In the next step, the sugar composition of the residues was determined according to the same procedure used for the starting material and tomato stem particles (Fig. 5). Sugars represented 39.8 % of the starting material (Table 3), and the weight fraction of tomato was 30 % in all the composites. Thus, the maximum sugar content in the composites was 11.9 % and the total amount quantified in the control samples was consistent with this value.

When the samples were not ground before the addition of enzymes (Fig. 5A), the total sugar content decreased very slightly, and the main loss was observed for glucose. When the samples were ground to 2 mm before degradation (Fig. 5B), the loss of sugar was more important than expected. Grinding increased the specific surface area and therefore the accessibility of enzymes. The greatest loss was observed in the tomato/PBS sample (- 2.85 %), which was mainly due to the release of glucose and galacturonic acid, in line with the main activities present in the selected enzyme cocktails. Once PHA was added to the polymer matrix, the release of sugars decreased to 1.95 %, which was similar to what was observed for the other polymer mixes.

In parallel, the composite degradation was followed by tomography analysis where porosity development was expected. Images of a unique piece of specimen were acquired after 0, 3 or 6 weeks of treatment, allowing to compare exactly the successive views. The level of porosity was calculated after each step of treatment (Table 6). Interestingly, all the samples subjected to enzymatic treatment exhibited the largest increase in the volume fraction porosity. For the controls and for all formulations (PBS, PBAT/PHA and PBAT/PLA), the increased porosity was mainly due to a debonding between the tomato stem particles and the polymer, and to the surface erosion of the polymer matrix (red arrows in Fig. 6A). After enzymatic treatment, the increase in porosity was due to the same phenomenon and also to the degradation of the polymer and tomato inside the specimen (green arrows in Fig. 6A).

After 3 weeks of degradation (treatment #1), the increase in the porosity of the PBS specimen was the greatest, in accordance with the release of sugars. Conversely, after 6 weeks of degradation, the porosity value was much greater in the PBAT/PLA sample. Fig. 6B shows the cumulative evolution of porosity at the edge (approximately 1 mm deep) and in the core of each specimen. The evolution of the cumulative porosity was the most important in the PBAT/PLA sample (1 %/mm on average), nearly double that of the other samples (0.6 %/mm on average for PBS; 0.4 %/mm on average for PBAT/PHA). When the sample contained PBS and PHA, the porosity increased 5-fold at the edge of the specimen compared with that in the center. Conversely, there was little difference in the cumulative porosity between the edge and center of the PBAT/PLA sample. The porosity of the PBAT/PLA specimens increased from 0.41 % to 4.41 % in the absence of enzymes, and from 0.32 % to 6.11 % after treatment with enzymes. These values are approximately twice as high as those in PBS and PBAT/PHA matrix.

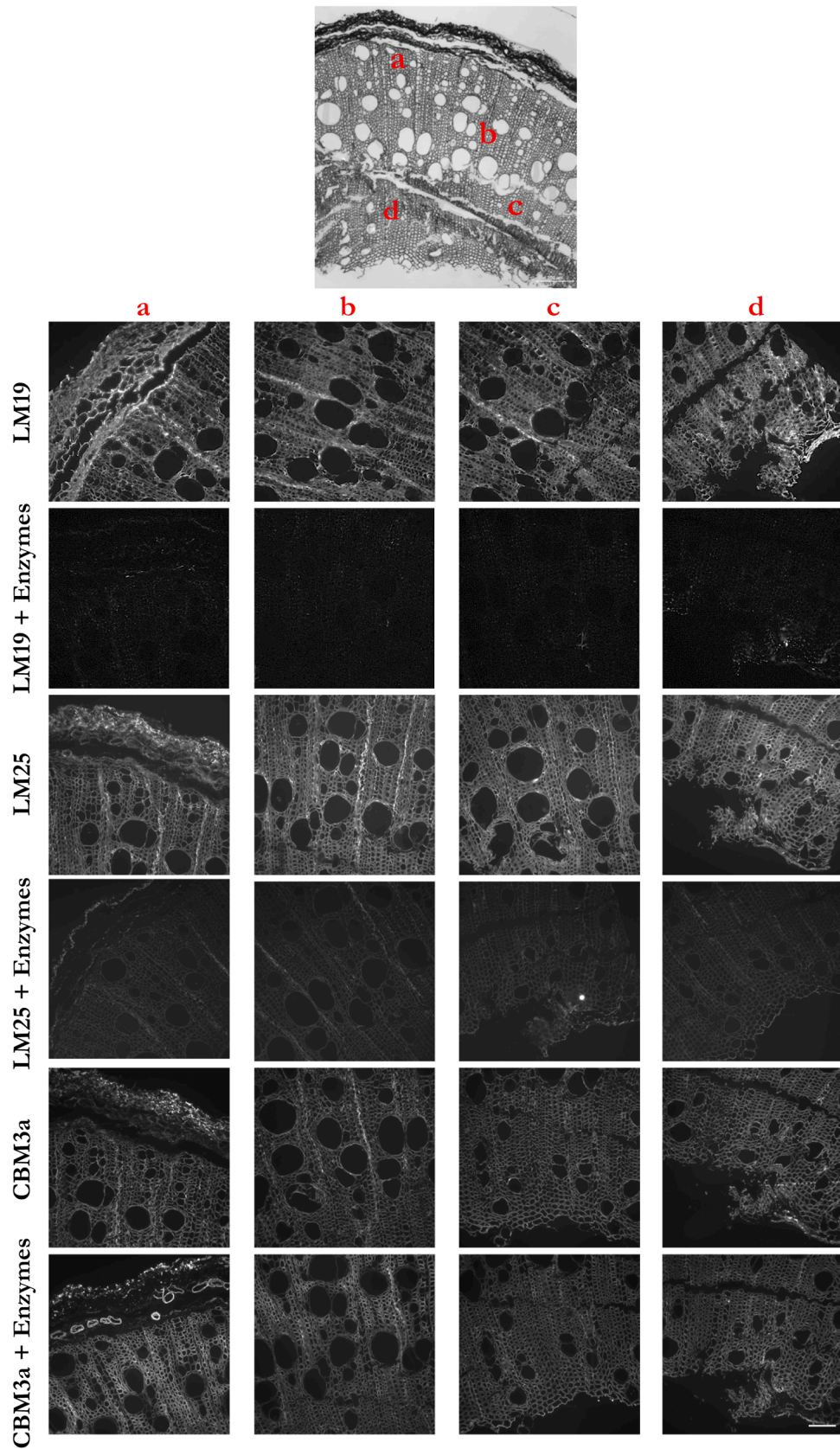


Fig. 3. Immunolabeling of tomato stem sections before and after enzymatic treatment. The insert shows the a, b, c, and d positions of the micrographs in the respective columns. LM19, LM25 and CBM3a are the probes used for labeling; see Section 3.2 for their respective specificities. Scale bar = 100 μ m.

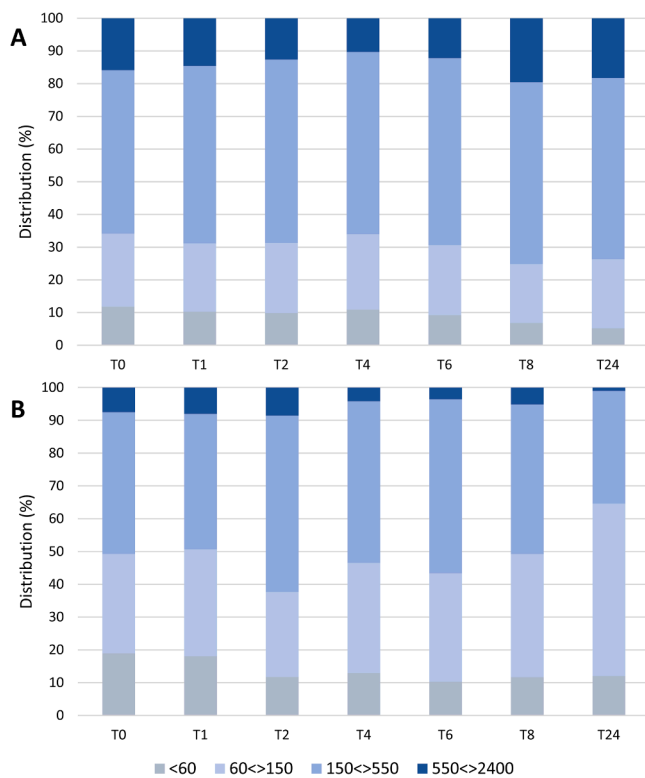


Fig. 4. Size distribution of tomato stem particles during enzymatic treatment with a mixture of Cellic CTech2 and Rapidase Fiber. A, control; B, in the presence of enzymes.

These results are in accordance with the work of [Pantaloni et al. \(2020\)](#), who showed that PBS and PHA polymers are eroded on the surface with an unclear evolution of porosity, and that the PLA sample showed the most important increase in volume porosity. The rapid degradation of PLA was attributed to the interface with the flax fibers in the core of the specimen. This phenomenon is particularly remarkable for the PBS- and PBAT/PHA-containing samples ([Fig. 6B](#)), which exhibit a strong degradation on the edges of the specimen. The evolution of the porosity through the specimen confirmed that the mechanism of degradation was different between PLA and the two other matrices. One of the main differences between PLA and the other polymers studied here is its relatively high glass transition temperature (T_g) (61 °C vs. negative values for the others; [Pantaloni et al., 2020](#)). As the degradation was carried out at 40 °C, PLA remained relatively stiff compared to the other polymers. During the degradation, liquid absorption causes the tomato stem particles to swell. Due to its high stiffness, PLA is unable to deform, and cracks may form. In contrast soft polymers such as PBAT or PBS can easily absorb the deformation and stress induced by fiber swelling.

In addition, a synergistic effect of plant fibers on PLA degradation

Table 5

Yields of solubilization of composite samples after 3 weeks of immersion in buffer (= Control) or the enzyme combination Cellic CTech2 and Rapidase Fiber (= Enz). The results are expressed in %.

| Polymer | Sample | Polymers alone | | Tomato stem, not ground | | Tomato stem, ground | |
|--------------|---------|----------------|------|-------------------------|-----|---------------------|------|
| | | Solubilization | SD | Solubilization | SD | Solubilization | SD |
| PBS | Control | 0.50 | 0.05 | 5.9 | 0.2 | 8.7 | 1.3 |
| | Enz | 0.52 | 0.10 | 5.3 | 0.8 | 10.7 | 0.6 |
| PBAT60/PHA40 | Control | 1.93 | 0.38 | 7.3 | 0.3 | 8.1 | 0.9 |
| | Enz | 0.54 | 0.17 | 7.9 | 0.6 | 10.7 | 0.8 |
| PBAT60/PLA40 | Control | 0.90 | 0.70 | 8.7 | 0.3 | 9.4 | 0.01 |
| | Enz | 0.57 | 0.02 | 9.0 | 0.3 | 13.3 | 0.5 |

SD = standard deviation, $n = 3$.

has also been suggested. In a previously published work ([Karimi-Avargani et al., 2020](#)), a composite PLA-jute was subjected to degradation by *Aspergillus flavus* secretome and compared to PLA alone.

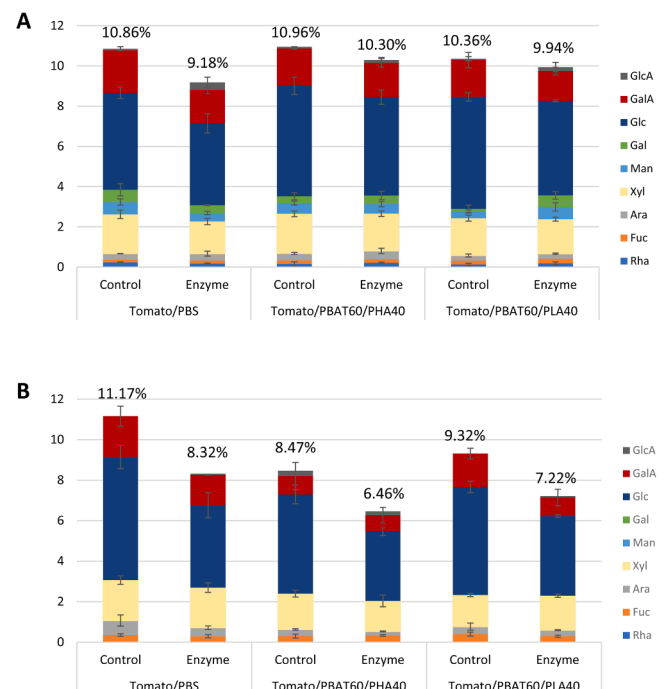


Fig. 5. Sugar composition of the composite material residues recovered after 3 weeks enzymatic degradation of A) unground and B) ground composite samples. The results are expressed as the percentage of dry matter. The values at the top of each bar are the total sugars.

Table 6

Evolution of the volume fraction porosity (%) based on the tomography characterization of the composite specimen containing 30 % tomato stem particles, before treatment, after 3 weeks of treatment (treatment #1) and after 6 weeks of treatment (treatment #2). The values in brackets correspond to the increase in porosity, expressed as a percentage of the starting value.

| Polymer | Sample | Porosity (%vol) | | |
|--------------|---------|------------------|--------------------|--------------------|
| | | before treatment | after treatment #1 | after treatment #2 |
| PBS | Control | 0.48 | 1.2 (+ 142 %) | 1.3 (+ 171 %) |
| | Enzyme | 0.28 | 2.7 (+ 853 %) | 3.7 (+ 1221 %) |
| PBAT60/PHA40 | Control | 0.30 | 1.3 (+ 333 %) | 1.7 (+ 466 %) |
| | Enzyme | 0.35 | 1.8 (+ 417 %) | 2.6 (+ 643 %) |
| PBAT60/PLA40 | Control | 0.32 | 1.5 (+ 369 %) | 4.4 (+ 1275 %) |
| | Enzyme | 0.41 | 2.2 (+ 427 %) | 6.1 (+ 1388 %) |

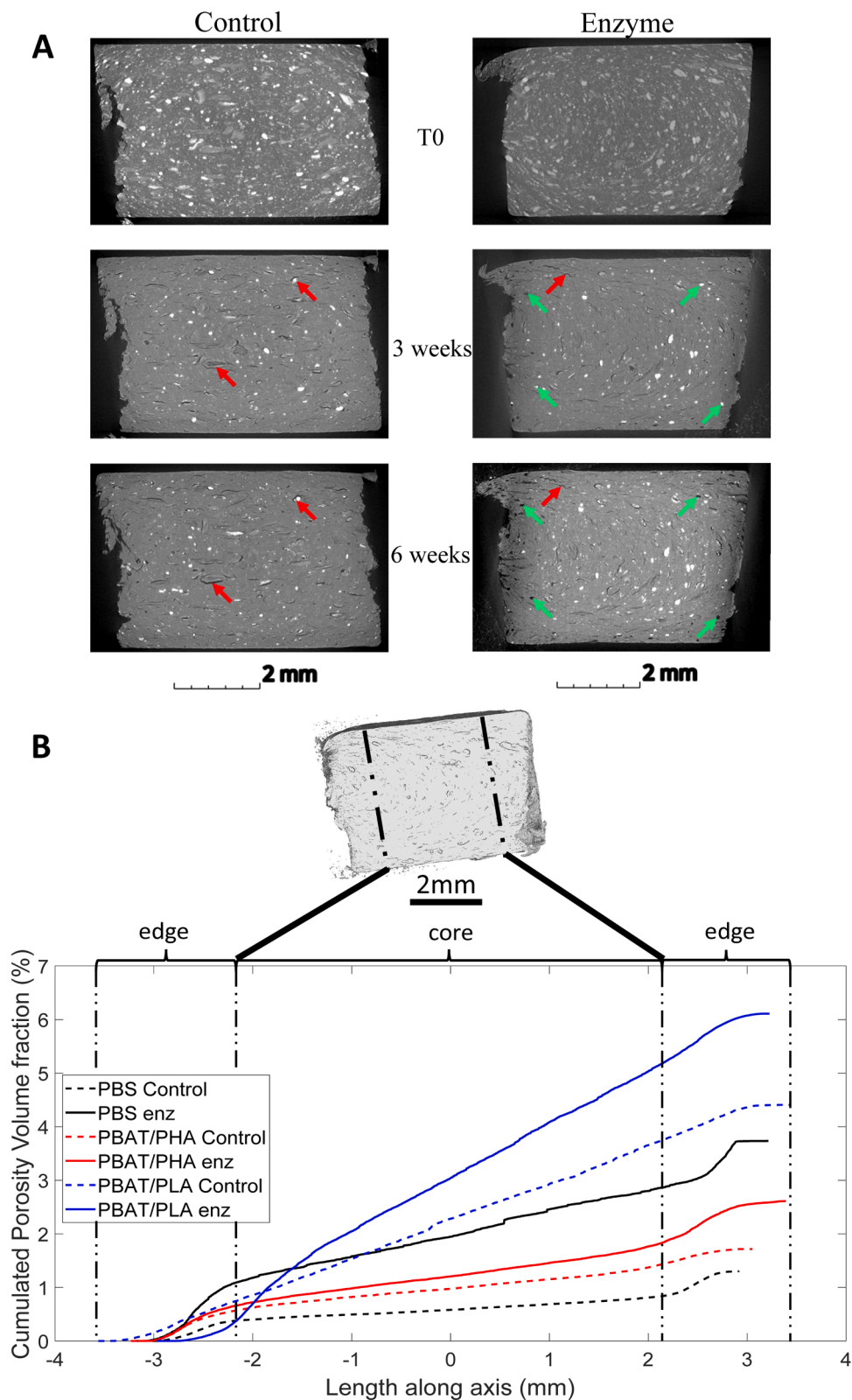


Fig. 6. A) Tomography images of PBAT/PLA/tomato stem samples after 0-, 3- or 6-weeks treatment without (Control) or with enzymes. Red arrows show particle-polymer debonding while the green arrows show the appearance of porosity due to degradation. B) Evolution of the cumulative porosity volume fraction with respect to the thickness of the specimens. The vertical dotted lines delimit the edge and core of the samples.

The authors observed a more intensive degradation of the PLA in the PLA-jute composite than in the PLA sample and attributed this observation to the promiscuous activity of the enzymes on plant fiber degradation, that could accelerate the PLA hydrolysis. As one of the enzymatic cocktails used in the present study was produced by *Aspergillus niger*, it can be hypothesized that a similar phenomenon occurred.

Conclusion

This work demonstrated that tomato stem particles are highly degradable by a range of suitable enzymes. These selected enzymes operate specifically on the cell wall polysaccharides present in the biomass, although no pre-treatment was applied. When the tomato biomass is incorporated in thermoplastic matrices such as PBS, PBAT or PLA to produce composite specimen, the enzymatic treatment induces a loss of weight, with a concomitant solubilization of polysaccharides and an increase of porosity in the degraded pieces. Altogether, this allows concluding that the tomato biomass is still degradable when embedded in a polymer matrix, the PBAT/PLA blend being the most favorable. As expected, composite specimens containing tomato stem particles were more degradable if previously ground, in relation to the increase of accessibility. This demonstrates the need for particle size control for further composting applications. Altogether, the results presented here pave the way for up-cycling post-harvest tomato plants into biodegradable composites usable to produce environmentally-friendly greenhouse accessories.

To assess the end-of-life composting potential of tomato stem-containing composites, further work is necessary to better understand the detailed degradation mechanism in the presence of composting-consortia microorganisms, notably by the specific monitoring of porosity propagation during the degradation stage. These new composites will combine satisfactory mechanical properties, biodegradability and environmental benefits by using tomato industrial by-products available in large quantities.

CRedit authorship contribution statement

Estelle Bonnin: Writing – review & editing, Writing – original draft, Project administration, Investigation, Funding acquisition, Data curation, Conceptualization. **Méline Calatraba:** Writing – review & editing, Methodology, Investigation, Formal analysis. **Xavier Gabrion:** Writing – review & editing, Writing – original draft, Methodology, Investigation, Formal analysis. **Camille Alvarado:** Writing – review & editing, Methodology, Investigation. **Coralie Buffet:** Writing – review & editing, Investigation, Formal analysis. **Arnaud Day:** Writing – review & editing, Resources. **Léna Brionne:** Writing – review & editing, Methodology. **Alain Bourmaud:** Writing – review & editing, Writing – original draft, Project administration, Investigation, Funding acquisition, Conceptualization. **Johnny Beaugrand:** Writing – review & editing, Project administration, Investigation, Funding acquisition, Conceptualization.

Declaration of competing interest

The authors declare that they have no known competing financial interests or personal relationships that could have appeared to influence the work reported in this paper.

Funding

This research was funded by FEDER and Région Pays de la Loire, France [grant number FEDER-FSE-2014–2020 09223], and by the PEPR-BBest project Filling Gaps [grant number ANR-22-PEBB-0006].

Acknowledgements

The authors are grateful to the MIFHySTO technological platform

(FEMTO-ST, Besançon, France) for the use of X-ray nanotomography.

The authors thank Basile Gautherot (COE of the CAVI company, France) for providing tomato stem samples as well as for fruitful discussions.

Data availability statement

Data supporting the findings of this study are available on simple request from the corresponding author.

Supplementary materials

Supplementary material associated with this article can be found, in the online version, at [doi:10.1016/j.clcb.2025.100136](https://doi.org/10.1016/j.clcb.2025.100136).

References

- Al-Furjan, M.S.H., Shan, L., Shen, X., Zarei, M.S., Hajmohammad, M.H., Kolahchi, R., 2022. A review on fabrication techniques and tensile properties of glass, carbon, and Kevlar fiber reinforced polymer composites. *J. Mater. Res. Technol.* 19, 2930–2959. <https://doi.org/10.1016/j.jmrt.2022.06.008>.
- Beaugrand, J., Guessasma, S., Maigret, J.-E., 2017. Damage mechanisms in defected natural fibers. *Scien. Rep.* 7 (1), 14041. <http://www.nature.com/articles/s41598-017-14514-6>.
- Blumenkrantz, N., Asboe-Hansen, G., 1973. New method for quantitative determination of uronic acids. *Anal. Biochem.* 54, 484–489.
- Bonnin, E., Garnier, C., Ralet, M.-C., 2014. Pectin-modifying enzymes and pectin-derived materials: applications and impacts. *Appl. Microbiol. Biotechnol.* 98 (2), 519–532. <https://doi.org/10.1007/s00253-013-5388-6>.
- Bourmaud, A., Pinsard, L., Guillou, E., De Luycker, E., Fazzini, M., Perrin, J., Weitkamp, T., Ouagne, P., 2022. Elucidating the formation of structural defects in flax fibres through synchrotron X-ray phase-contrast microtomography. *Indus. Crops Prod.* 184, 115048. <https://doi.org/10.1016/j.indcrop.2022.115048>.
- Bourmaud, A., Korschak, K., Buffet, C., Calatraba, M., Rudolph, A.L., Kervoelen, A., Gautherot, B., Bonnin, E., Beaugrand, J., 2023. A circular approach for the valorization of tomato by-product in biodegradable injected materials for horticulture sector. *Polymers (Basel)* 15, 820.
- Coroller, G., Lefeuvre, A., Le Duigou, A., Bourmaud, A., Ausias, G., Gaudry, T., Baley, C., 2013. Effect of flax fibres individualisation on tensile failure of flax/epoxy unidirectional composite. *Compos. Part A Appl. Sci. Manuf.* 51, 62–70. <https://doi.org/10.1016/j.compositesa.2013.03.018>.
- Deram, P., Lefsrud, M.G., Orsat, V., 2014. Supplemental lighting orientation and red-to-blue ratio of light-emitting diodes for greenhouse tomato production. *HortScience* 49 (4), 448–452. <https://doi.org/10.21273/hortsci.49.4.448>.
- El Hage, F., Legland, D., Borrega, N., Jacquemot, M.P., Griveau, Y., Coursol, S., Méchin, V., Reymond, M., 2018. Tissue lignification, cell wall p-coumaroylation and degradability of maize stems depend on water status. *J. Agric. Food Chem.* 66 (19), 4800–4808.
- Englyst, H.N., Cummings, J.H., 1988. Improved method of measurement of dietary fiber as non-starch polysaccharides in plant foods. *J. Assoc. Off. Anal. Chem.* 71 (4), 808–814.
- Eurostat, 2024. https://ec.europa.eu/eurostat/databrowser/view/apro_cpsh1_custom_8748007/default/table.
- Fukushima, R.S., Hatfield, R.D., 2001. Extraction and isolation of lignin for utilization as a standard to determine lignin concentration using the acetyl bromide spectrophotometric method. *J. Agric. Food Chem.* 49 (7), 3133–3139.
- Garcea, S.C., Wang, Y., Withers, P.J., 2018. X-ray computed tomography of polymer composites. *Compos. Sci. Technol.* 156, 305–319. <https://doi.org/10.1016/j.compscitech.2017.10.023>.
- Jiang, Y., Lawrence, M., Ansell, M.P., Hussain, A., 2018. Cell wall microstructure, pore size distribution and absolute density of hemp shiv. *Roy. Soc. Open Sci.* 5 (4), 171945. <https://royalsocietypublishing.org/doi/10.1098/rsos.171945>.
- Jung, H.-W., Yang, M.-K., Su, R.-C., 2018. Purification, characterization, and gene cloning of an *Aspergillus fumigatus* polyhydroxybutyrate depolymerase used for degradation of polyhydroxybutyrate, polyethylene succinate, and polybutylene succinate. *Polym. Deg. Stab.* 154, 186–194.
- Karimi-Avargani, M., Bazooyar, F., Biria, D., Zamani, A., Skrifvars, M., 2020. The special effect of the *Aspergillus flavus* and its enzymes on biological degradation of the intact polylactic acid (PLA) and PLA-jute composite. *Polym. Deg. Stab.* 179, 109295.
- Kelly, A., Tyson, W.R., 1965. Tensile properties of fibre-reinforced metals: copper/tungsten and copper/molybdenum. *J. Mech. Phys. Solids* 13, 329–338.
- Le Duigou, A., Davies, P., Baley, C., 2011. Environmental impact analysis of the production of flax fibres to be used as composite material reinforcement. *J. Biobased Mater. Bioener.* 5, 1–13.
- Manriquez-Altamirano, A., Sierra-Pérez, J., Muñoz, P., Gabarrell, X., 2021. Identifying potential applications for residual biomass from urban agriculture through eco-ideation: tomato stems from rooftop greenhouses. *J. Clean. Prod.* 295, 126360. <https://doi.org/10.1016/j.jclepro.2021.126360>.
- Melelli, A., Pantalonì, D., Balnois, E., Arnould, O., Jamme, F., Baley, C., Beaugrand, J., Shah, D.U., Bourmaud, A., 2021. Investigations by AFM of ageing mechanisms in

- PLA-Flax fibre composites during garden composting. *Polymers*. (Basel) 13 (14), 2225. <https://doi.org/10.3390/polym13142225>.
- Mongioli, C., Lacalamita, D., Morin-Crini, N., Gabrion, X., Ivanovska, A., Sala, F., Placet, V., Rizzi, V., Gubitosa, J., Mesto, E., Ribeiro, A.R.L., Fini, P., Vietro, N.D., Schingaro, E., Kostić, M., Cosentino, C., Cosma, P., Bradu, C., Chanet, G., Crini, G., 2021. Use of Chênevotte, a valuable co-product of industrial hemp fiber, as adsorbent for pollutant removal. Part I: chemical, microscopic, spectroscopic and thermogravimetric characterization of raw and modified samples. *Molecules*. 26 (15), 4574.
- Mongioli, C., Crini, G., Gabrion, X., Placet, V., Blondeau-Patissier, V., Krystianiak, A., Durand, S., Beaugrand, J., D'Orlando, A., Rivard, C., Gautier, L., Ribeiro, A.R.L., Lacalamita, D., Martel, B., Staelens, J.-N., Ivanovska, A., Kostić, M., Heintz, O., Bradu, C., Raschetti, M., Morin-Crini, N., 2022. Revealing the adsorption mechanism of copper on hemp-based materials through EDX, nano-CT, XPS, FTIR, Raman, and XANES characterization techniques. *Chem. Eng. J. Adv.* 10, 100282. <https://doi.org/10.1016/j.cej.2022.100282>.
- Nistico, R., Evon, P., Labonne, L., Vaca-Medina, G., Montoneri, E., Vaca-Garcia, C., Negre, M., 2017. Post-harvest tomato plants and urban food wastes for manufacturing plastic films. *J. Clean. Prod.* 167, 68–74. <https://doi.org/10.1016/j.jclepro.2017.08.160>.
- Nuez, L., Gautreau, M., Mayer-Laigle, C., D'Arras, P., Guillon, F., Bourmaud, A., Baley, C., Beaugrand, J., 2020. Determinant morphological features of flax plant products and their contribution in injection moulded composite reinforcement. *Compos. Part C: Open Access* 3, 100054. <https://doi.org/10.1016/j.jcomc.2020.100054>.
- Pantaloni, D., Shash, D., Baley, C., Bourmaud, A., 2020. Monitoring of mechanical performances of flax non-woven biocomposites during a home compost degradation. *Polym. Deg. Stab.* 177, 109166. <https://doi.org/10.1016/j.polymdegradstab.2020.109166>.
- Pemas, S., Gkiliopoulos, D., Samiotaki, C., Bikiaris, D.N., Terzopoulou, Z., Pechlivani, E. M., 2024. Valorization of tomato agricultural waste for 3D-printed polymer composites based on poly(lactic acid). *Polymers*. (Basel) 16 (11), 1536. <https://doi.org/10.3390/polym16111536>.
- Quereilhac, D., Pinsard, L., Guillou, E., Fazzini, M., De Luycker, E., Bourmaud, A., Abida, M., Perrin, J., Weitkamp, T., Ouagne, P., 2023. Exploiting synchrotron X-ray tomography for a novel insight into flax-fibre defects ultrastructure. *Indus. Crops Prod* 198, 116655.
- Rani, M., Choudhary, P., Krishnan, V., Zafar, S., 2021. A review on recycling and reuse methods for carbon fiber/glass fiber composites waste from wind turbine blades. *Compos. Part B Eng.* 215, 108768. <https://doi.org/10.1016/j.compositesb.2021.108768>.
- Santos-Pereira, C., Sousa, J., Costa, A.M.A., Santos, A.O., Rito, T., Soares, P., Franco-Duarte, R., Silvério, S.C., Rodrigues, L.R., 2023. Functional and sequence-based metagenomics to uncover carbohydrate-degrading enzymes from composting samples. *Appl. Microbiol. Biotechnol.* 107 (17), 5379–5401.
- Scaffaro, R., Citarrella, M.C., Morreale, M., 2023. Green composites based on Mater-Bi® and *Solanum lycopersicum* plant waste for 3D printing applications. *Polymers*. (Basel) 15 (2), 325. <https://doi.org/10.3390/polym15020325>.
- Scaffaro, R., Gulino, E.F., Citarrella, M.C., 2024. Multifunctional 3D-printed composites based on biopolymeric matrices and tomato plant (*Solanum lycopersicum*) waste for contextual fertilizer release and Cu(II) ions removal. *Adv. Compos. Hybrid Mater.* 7 (3), 95. <https://doi.org/10.1007/s42114-024-00908-4>.
- Shadhin, M., Rahman, M., Jayaraman, R., Chen, Y., Mann, D., Zhong, W., 2023. Natural biomass & waste biomass fibers – Structures, environmental footprints, sustainability, degumming methods, & surface modifications. *Indus. Crops Prod* 204, 117252.
- Thibault, J.-F., 1979. Automatisation du dosage des substances pectiques par la méthode au méta-hydroxydiphényl. *Lebensmitt. Wissensch. Technol.* 12, 247–251.
- Torabizadeh, H., 2011. All proteins have a basic molecular formula. *Inter. J. Chem., Mol., Nucl. Metal. Eng.* 5 (6), 501–505.
- Varnai, A., Huikko, L., Pere, J., Siika-aho, M., Viikari, L., 2011. Synergistic action of xylanase and mannanase improves the total hydrolysis of softwood. *Biores. Technol.* 102 (19), 9096–9104.
- Yadav, S.K., 2017. Technological advances and applications of hydrolytic enzymes for valorization of lignocellulosic biomass. *Biores. Technol.* 245, 1727–1739.
- Zwanenburg, E.A., Norman, D.G., Qian, C., Kendall, K.N., Williams, M.A., Warnett, J.M., 2023. Effective X-ray micro computed tomography imaging of carbon fibre composites. *Compos. Part B: Eng.* 258, 110707. <https://doi.org/10.1016/j.compositesb.2023.110707>.